A Reach Control Approach to Bumpless Transfer of Robotic Manipulators

Matthew Martino and Mireille E. Broucke

***Abstract*— We present a novel control method based on *reach controllers* to make the end effector of a robotic manipulator reach and maintain contact with an environment without inducing bouncing or switching between the reach control and force control modalities.**

I. Introduction

This paper presents a novel control design method for making the end effector of a manipulator reach and maintain contact with a solid object in its workspace. This maneuver involves a transition from position control to force control and the key requirement is for this transition to occur only once, preventing *bouncing* or switching of the control modality. While the modelling for this problem is based on standard concepts [12], the control design instead relies on a novel design methodology using so-called *reach controllers* [5], [6], [11], [1], [2]. The method is presented for a two link manipulator, but it generalizes to more general manipulators.

Previous work on bumpless transfer of a manipulator includes [13], [7], [14], [3], [10]. The present work is most closely related to [3]. Both approaches use Lyapunov analysis to construct invariant sets in which trajectories must enter under position control in order to guarantee that the velocity at impact is below a threshhold. Unlike [3], here we assume that the parameters of the environment are not precisely known. We also obtain a larger set of initial conditions from which to initiate the manipulator.

Notation. The notation $\mathrm{co}\{\, v_1, v_2, \ldots\}$ denotes the convex hull of points $v_1, v_2, \ldots \in \mathbb{R}^n$. For $x, y \in \mathbb{R}^n$, $x \cdot y$ denotes the inner product of x and y. Notation $\mathbf{0}$ denotes a zero vector of appropriate dimension. The paper assumes some background on simplices, polytopes, triangulations, and piecewise affine feedback. See [5].

II. Modelling

Consider the system illustrated in Figure 1 consisting of a two link manipulator. A mass m_2 is attached to the end effector of the manipulator through a spring. Let (x_1, y_1) and (x_2, y_2) be the position (with respect to the base frame) of the end effector of the manipulator and of the second mass, respectively. It is typical to feedback linearize the nonlinear manipulator model to obtain a linear model in the end effector position (x_1, y_1) [12]. Here we make two simplifying assumptions. First, we assume that the second mass only moves horizontally. The equations of motion for

The authors are with the Department of Electrical and Computer Engineering, University of Toronto, Toronto, ON M5S 3G4, Canada (e-mail: broucke@control.utoronto.ca). Supported by the Natural Sciences and Engineering Research Council of Canada (NSERC).

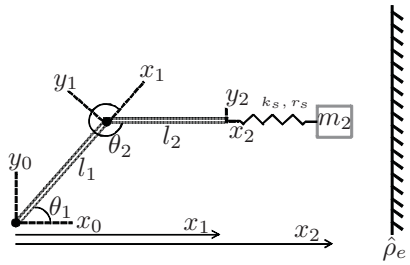

Fig. 1: Two-link Manipulator with second mass m_2.

the x-dynamics only are

$$m_1\ddot{x}_1 = f_s + u \tag{1a}$$
$$m_2\ddot{x}_2 = -f_s + f_e\,, \tag{1b}$$

where $u \in \mathbb{R}$ is the input, $f_s \in \mathbb{R}$ is the *sensed force*, and $f_e \in \mathbb{R}$ is the *environment force*. The sensed force is modelled as a virtual spring with spring constant k_s and rest length r_s as follows

$$f_s = k_s(x_2 - x_1 - r_s)\,. \tag{2}$$

Similarly, the external force f_e acts along the x-axis on the second mass only when it is in contact with an obstacle located at $(\hat{\rho}_e, 0)$. Thus,

$$f_e = \begin{cases} k_e(\hat{\rho}_e - x_2) & x_2 \geq \hat{\rho}_e \\ 0 & x_2 < \hat{\rho}_e\,. \end{cases} \tag{3}$$

It is assumed that the exact value of k_e is unknown but it is bounded within a known range given by $k_e \in [k_{emin}, k_{emax}]$. Similarly, the exact value of $\hat{\rho}_e$ is unknown but lies in the range $[\hat{\rho}_{emin}, \hat{\rho}_{emax}]$.

The second simplification is that we reduce the two-mass model (1) to a single mass model by exploiting the fact that $m_1 >> m_2$. Substituting (2) and (3) in (1b), assuming that $\ddot{x}_2 \simeq 0$ during contact, and solving for x_2, we get

$$x_2 = \frac{1}{k_s + k_e}\Big[k_s(x_1 + r_s) + k_e\hat{\rho}_e\Big]\,. \tag{4}$$

Then we substitute (4) into (2) and simplify to get

$$f_s = \overline{k}(\hat{\rho}_e - r_s - x_1) \tag{5}$$

where $\overline{k} := \frac{k_s k_e}{k_s + k_e}$ is called the *effective spring constant*. Let $\xi = (x_1, \dot{x}_1)$. When there is no contact with the environment, the free motion of the first mass is given by

$$\dot{\xi} = \begin{bmatrix} 0 & 1 \\ 0 & 0 \end{bmatrix}\xi + \begin{bmatrix} 0 \\ \frac{1}{m_1} \end{bmatrix} u\,. \tag{6a}$$

The output of this model is the position of the second mass given by $x_2 = \xi_1 + r_s$. When there is contact with the

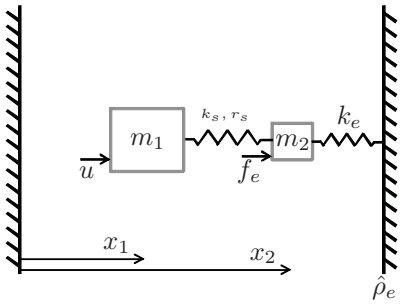

Fig. 2: Two-mass model consisting of the feedback-linearized manipulator, m_1, and second mass m_2.

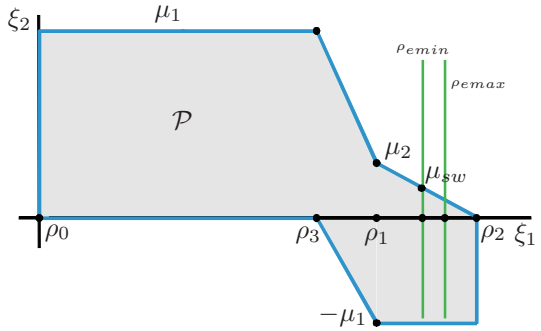

Fig. 3: The constrained state space of (ξ_1, ξ_2) according to the Complex Specifications.

environment, the single mass approximation of the two mass system is

$$\dot{\xi} = \begin{bmatrix} 0 & 1 \\ 0 & 0 \end{bmatrix} \xi + \begin{bmatrix} 0 \\ \frac{1}{m_1} \end{bmatrix} u + \begin{bmatrix} 0 \\ \frac{1}{m_1} \end{bmatrix} f_s \,. \tag{6b}$$

Based on (4), the output of this model is the position of the second mass given by

$$x_2 = \frac{1}{k_s + k_e} \left[k_s(\xi_1 + r_s) + k_e \hat{\rho}_e \right] . \tag{6c}$$

Finally, we require a model for the dynamics of the sensed force so that a suitable force controller may be designed for force regulation during contact with the environment. We take the second derivative of (5) and substitute the model (1a) to obtain the second-order force dynamics

$$m_1 \ddot{f}_s + \overline{k} f_s + \overline{k} u = 0 \,. \tag{6d}$$

We are interested in designing a force controller to stabilize f_s to some desired steady-state contact force, $f_s^d < 0$. A suitable PD controller is

$$u_f := -f_s + k_1 (f_s - f_s^d) + k_2 \dot{f}_s \tag{6e}$$

with parameters $k_1, k_2 > 0$ determining the closed-loop poles. Finally, by substituting (5) and (6e) into (1a), we obtain the state model for the closed-loop force dynamics when there is contact with the environment

$$\dot{\xi} = \begin{bmatrix} 0 & 1 \\ -\frac{\overline{k} k_1}{m_1} & -\frac{\overline{k} k_2}{m_1} \end{bmatrix} \xi + \begin{bmatrix} 0 \\ \frac{\overline{k} k_1 \rho_f^d}{m_1} \end{bmatrix} =: A\xi + a \tag{6f}$$

where

$$\rho_f^d := \hat{\rho}_e - r_s - \frac{f_s^d}{\overline{k}} \,. \tag{6g}$$

III. Logic Control Specifications

The control specifications will be presented in terms of the states ξ of the first mass. However, these ξ requirements can be translated to requirements on $(x_2, \dot{x}_2)$ for the second mass using the relationships $x_2 = \xi_1 + r_s$, $\dot{x}_2 = \xi_2$, and the constants $\rho_{emin} := \hat{\rho}_{emin} - r_s$, $\rho_{emax} := \hat{\rho}_{emax} - r_s$, and $\rho_e := \hat{\rho}_e - r_s$.

Problem 3.1: We consider the model (6a)-(6c) along with a force controller (6e). We are given the system parameters masses m_1 and m_2 with $m_1 >> m_2$; sensed force parameters k_s and r_s; the range for the environment spring constant, $k_e \in [k_{emin}, k_{emax}]$; the range for the effective spring constant, $\overline{k} \in [\overline{k}_{min}, \overline{k}_{max}]$; the range of the environment position $\hat{\rho}_e \in [\hat{\rho}_{emin}, \hat{\rho}_{emax}]$ where $0 \leq \hat{\rho}_{emin} \leq \hat{\rho}_{emax}$; and force controller parameters k_1, k_2, and f_s^d. Finally, we are given the specification parameters: ρ_i, $i = 0, \ldots, 3$, μ_{sw}, and μ_1. The measurements are the states of the first mass ξ and the sensed force f_s. The control objective is to find a state feedback such that the closed-loop system achieves the following specifications.

(S1) **Temporal Sequence**: The first mass starts at $\xi_1(0) \in [\rho_0, \rho_{emin})$ corresponding to non-contact of the second mass. Eventually it reaches a position ρ_e, corresponding to the second mass making contact. Then the second mass maintains contact with the environment.

(S2) **Safety**

- $\rho_0 \leq \xi_1 \leq \rho_2$ where $\rho_2 > \rho_{emax}$.
- $|\xi_2| \leq \mu_1$.
- If $\xi_1 \in [\rho_3, \rho_1]$ and $\xi_2 \geq 0$, then $(\mu_1 - \mu_2)\xi_1 + (\rho_1 - \rho_3)\xi_2 \leq \rho_1 \mu_1 - \rho_3 \mu_2$.
- If $\xi_1 \in [\rho_1, \rho_2]$ and $\xi_2 \geq 0$, then $\mu_{sw}\xi_1 + (\rho_2 - \rho_{emin})\xi_2 \leq \mu_{sw}\rho_2$.

(S3) **Liveness**

- If $\xi_1 \in [\rho_0, \rho_3]$, then $\xi_2 \geq 0$.
- If $\xi_1 \in [\rho_3, \rho_1]$ and $\xi_2 \leq 0$, then $\mu_1 \xi_1 + (\rho_1 - \rho_3)\xi_2 \geq \mu_1 \rho_3$.

Of particular importance is the fourth safety specification that restricts the maximum allowed relative velocity at impact between the second mass and the environment. Assuming that the environment is stationary but lies at a distance between $[\hat{\rho}_{emin}, \hat{\rho}_{emax}]$, the maximum relative velocity at impact can be derived from the fourth safety constraint by solving for ξ_2 to obtain $\xi_2 \leq \mu_{sw} \frac{\rho_2 - \xi_1}{\rho_2 - \rho_{emin}}$. It is evident from the formula that the maximum relative velocity at impact is μ_{sw} when the first mass is at $\xi_1 = \rho_{emin}$. The liveness requirements of (S3) force the first mass to move toward the environment in a lively way when it is sufficiently far and to only move backwards as far as ρ_3.

IV. Methodology

The linear inequality constraints comprising the safety and liveness specifications define a state space which is a non-convex polytope, denoted $\mathcal{P}$. This polytope can be visualised

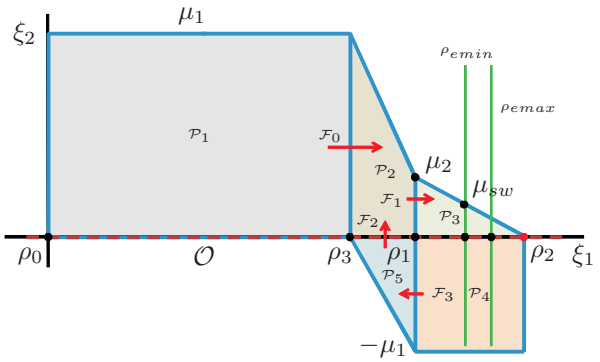

Fig. 4: The subdivision of $\mathcal{P}$ and intended directions of travel across *exit facets* $\mathcal{F}_i$.

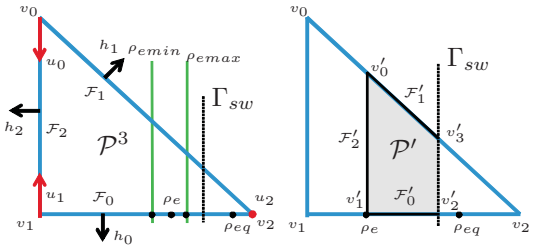

Fig. 5: Salient variables for region $\mathcal{P}^3$, and the polytope $\mathcal{P}'$ in the proof of Lemma 4.1.

in the ξ-plane as in Figure 3. The vertical band delimited by the (green) vertical lines indicates the range of positions of the environment. Satisfaction of the temporal sequence corresponds to closed-loop trajectories moving to the right in $\mathcal{P}$. We divide the state space $\mathcal{P}$ into five regions, $\mathcal{P}^i$, $i = 1, \ldots, 5$, as seen in Figure 4, and we specify on each region a suitable closed-loop behavior to achieve the overall specification. The closed-loop behavior of each region will be achieved using a piecewise affine feedback based on the theory of *reach controllers*; we refer the reader to the extensive literature on this subject [5], [6], [11], [2]. Here we only give the main idea of such controllers.

Referring to Figure 4, in region $\mathcal{P}^1$ a piecewise affine reach controller will be specified using the theory of [2] so that all trajectories initialized in $\mathcal{P}^1$ reach the exit facet $\mathcal{F}_0$ in finite time, corresponding to quick movement of the manipulator toward the environment; that is, $\mathcal{P}^1 \xrightarrow{\mathcal{P}^1} \mathcal{F}_0$. In region $\mathcal{P}^2$, whose shape corresponds to a rapid deceleration of the manipulator, a piecewise affine reach controller will be designed so that $\mathcal{P}^2 \xrightarrow{\mathcal{P}^2} \mathcal{F}_1$. The region $\mathcal{P}^3$, a simplex, will receive special treatment. Here a reach controller will be specified to drive trajectories to reach a set of states corresponding to contact with the environment, after which a force controller is activated. In Lemma 4.2 it is shown that the closed-loop system (6f) under the force controller (6e) can never return to a state corresponding to a reach control modality. In region $\mathcal{P}^4$ a piecewise affine reach controller will be designed so that $\mathcal{P}^4 \xrightarrow{\mathcal{P}^4} \mathcal{F}_3$ and similarly on $\mathcal{P}^5$ we require $\mathcal{P}^5 \xrightarrow{\mathcal{P}^5} \mathcal{F}_2$. Region $\mathcal{P}^5$ corresponds to the manipulator decelerating away from the environment in order to set up another approach to it in region $\mathcal{P}^2$.

Assumption 4.1: For the force controller (6e), we assume k_1 and k_2 are such that for all $\overline{k} \in [\overline{k}_{min}, \overline{k}_{max}]$, A defined in (6f) is Hurwitz.

Suppose that a switching force $f_{sw} \leq 0$ is specified corresponding to when force control must be initiated. Let ρ_{sw} be the position of the first mass corresponding to a sensed force of $f_s = f_{sw}$ under the dynamics (6b). This position (in analogy with (6g) relating the desired force and its corresponding position) is given by

$$\rho_{sw} := \rho_e + \frac{|f_{sw}|}{\overline{k}}. \tag{7}$$

Observe that by definition $\rho_{sw} \geq \rho_e$, so the switching position corresponds to mass two being in contact with the environment. We also define the *switching boundary* $\Gamma_{sw}(\overline{k})$ in $\mathcal{P}^3$ by

$$\Gamma_{sw}(\overline{k}) := \left\{ \xi \in \mathcal{P}^3 \mid \xi_1 = \rho_{sw} \right\}. \tag{8}$$

Let $\mathcal{P}^3 = \text{co}\{v_0, v_1, v_2\}$ where $v_0 = (\rho_1, \mu_2)$, $v_1 = (\rho_1, 0)$, and $v_2 = (\rho_2, 0)$, where $\rho_1 < \rho_2$ and $\mu_2 > 0$. Also, the environment position lies in $\mathcal{P}^3$; that is, $\rho_1 < \rho_{emin} \leq \rho_e \leq \rho_{emax} < \rho_2$. See Figure 5. We choose $\rho_2 > \rho_{emax} + \frac{|f_{sw}|}{k_{min}} \geq \rho_{sw}$.

We first design a reach controller for the non-contact system (6a) that drives its trajectories to v_2. Since $v_2 = (\rho_2, 0)$, this places v_2 to the right of ρ_{emax}. Consequently contact will be made with the environment and moreover, a sufficiently high contact force is induced to allow states to reach $\Gamma_{sw}(\overline{k})$.

Lemma 4.1: Consider the simplex $\mathcal{P}^3$ and systems (6a)-(6c), where $\overline{k} \in [\overline{k}_{min}, \overline{k}_{max}]$, and $\hat{\rho}_e \in [\hat{\rho}_{emin}, \hat{\rho}_{emax}]$. There exists an affine feedback $u = K\xi + g$ such that:

(i) For system (6a), the closed-loop trajectories satisfy: for all $\xi_0 \in \mathcal{P}^3$, $\phi(t, \xi_0) \in \mathcal{P}^3$ for all $t \geq 0$. Moreover, $\lim_{t\to\infty} \phi(t, \xi_0) = v_2$.

(ii) For system (6b), the closed-loop trajectories satisfy: for all $\xi_0 \in \{\xi \in \mathcal{P}^3 \mid \rho_e < \xi_1 < \rho_{sw}\}$, $\phi(t, \xi_0)$ reaches $\Gamma_{sw}(\overline{k})$ in finite time.

Proof: First we prove (i). We select control values at the vertices of $\mathcal{P}^3$ satisfying $u_0 < 0$, $u_2 = 0$, and

$$u_1 > \frac{|f_{sw}|(\rho_2 - \rho_1)}{\left(\rho_2 - \rho_{emax} - \frac{|f_{sw}|}{\overline{k}_{min}}\right)} > 0. \tag{9}$$

The particular form of (9) will be explained in the proof of (ii) below. Using equation (8) of [5], one can synthesize the affine feedback $u = K\xi + g$. It can be verified that $h_j \cdot (Av_i + Bu_i + a) \leq 0$, $i \in \{0, 1, 2\}$ and $j \in \{0, 1, 2\} \setminus \{i\}$. By convexity of the closed-loop vector field, these statements imply the vector field points inside $\mathcal{P}^3$ at all points on its boundary. It follows by a standard argument that for all $\xi_0 \in \mathcal{P}^3$, $\phi(t, \xi_0) \in \mathcal{P}^3$ for all $t \geq 0$. Evaluating the closed-loop system at the point v_2, one immediately verifies it is an equilibrium of the closed-loop system. Now we apply

Theorem 4.19 of [6] to show that all trajectories tend to v_2. There are two requirements[1]: (a) the vector field points inside $\mathcal{P}^3$ at all points on its boundary; (b) the closed-loop velocity vectors at the vertices of $\mathcal{P}^3$ span $\mathbb{R}^2$. We have already verified (a). For (b), we have $Av_0 + Bu_0 + a = (\mu_2, \frac{u_0}{m_1})$ and $Av_1 + Bu_1 + a = (0, \frac{u_1}{m_1})$, which span $\mathbb{R}^2$. We conclude $\lim_{t\to\infty} \phi(t, \xi_0) = v_2$.

Second we prove (ii). It can be shown (we omit the detailed calculation) that with the choice (9) the closed-loop system (6b) has only one equilibrium in $\mathcal{P}^3$ at $\xi_{eq} := (\rho_{eq}, 0) \in \mathcal{P}^3$ where $\rho_{sw} < \rho_{eq} < \rho_2$. Define the polytope $\mathcal{P}' := \text{co}\{v_0', v_1', v_2', v_3'\} \subset \mathcal{P}^3$ as depicted in Figure 5. The vertices are given by $v_0' = (\rho_e, \mu_e)$, $v_1' = (\rho_e, 0)$, $v_2' = (\rho_{sw}, 0)$, and $v_3' = (\rho_{sw}, \mu_{sw})$. Notice that $\Gamma_{sw}(\overline{k})$ forms the right edge of $\mathcal{P}'$. If we define facets of $\mathcal{P}'$ to be $\mathcal{F}_0' = \text{co}\{v_1', v_2'\}$, $\mathcal{F}_1' = \text{co}\{v_0', v_3'\}$, and $\mathcal{F}_2' = \text{co}\{v_0', v_1'\}$, then it can be shown that the closed-loop vector field for (6b) using the affine feedback given in part (i) points inward on $\mathcal{F}_0'$, $\mathcal{F}_1'$, and $\mathcal{F}_2'$. Because $\xi_{eq} \notin \mathcal{P}'$, it can be readily shown that $0 \notin \text{co}\{Av_1' + B(Kv_1' + g) + a, Av_2' + B(Kv_2' + g) + a\}$. Since $\mathcal{O} = \{\xi \in \mathbb{R}^2 \mid \xi_2 = 0\}$, we can apply Theorem 4.3 of [2] to conclude that all trajectories in $\mathcal{P}'$ reach $\Gamma_{sw}(\overline{k})$ in finite time. ■

Next we consider the system (6f) in contact with the environment. We show that if the force controller (6e) is initiated from states in $\mathcal{P}^3$ along the switching boundary $\Gamma_{sw}(\overline{k})$, then under the controller (6e) it is not possible for the state to return to a value with $\xi_1 < \rho_{sw}$ (although it is permitted for the state to exit $\mathcal{P}^3$). The result is actually obtained by appropriately placing the vertics of $\mathcal{P}^3$.

Let $\xi_f^d := (\rho_f^d, 0)$. It can be shown that (6f) is equivalent to $\dot{\xi} = A(\xi - \xi_f)$ where A is given in (6f). Suppose we are given f_{sw} with $|f_{sw}| < |f_s^d|$. We select $Q = \left[\begin{smallmatrix} Q_1 & Q_2 \\ Q_2 & Q_3 \end{smallmatrix}\right]$ to be symmetric and positive definite. Let $P = \left[\begin{smallmatrix} P_1 & P_2 \\ P_2 & P_3 \end{smallmatrix}\right]$ and define the Lyapunov function

$$\begin{aligned} V(\xi) &= (\xi - \xi_f^d)^T P(\xi - \xi_f^d) && (10) \\ &= P_1(\xi_1 - \rho_f^d)^2 + 2P_2(\xi_1 - \rho_f^d)\xi_2 + P_3\xi_2^2 . && (11) \end{aligned}$$

Substituting A given in (6f) and Q into the Lyapunov equation $A^TP + PA = -Q$, by Assumption 4.1, we get a symmetric, positive definite solution for P with

$$P_2 = \frac{Q_1 m_1}{2\overline{k}k_1}, \quad P_3 = \left(\frac{Q_1 m_1}{\overline{k}k_1} + Q_3\right)\frac{m_1}{2\overline{k}k_2} . \qquad (12)$$

It can be verified using (6f) that $\dot{V} = -(\xi - \xi_f^d)^T Q(\xi - \xi_f^d) < 0$ for $\xi \neq \xi_f^d$. We consider the level set of V given by $\{\xi \in \mathbb{R}^2 \mid V(\xi) = P_1(\rho_{sw} - \rho_f^d)\}$ that passes through the point $(\rho_{sw}, 0)$. This level set passes through a second point $(\rho_{sw}, \mu_Q(\overline{k}))$ along the line $\xi_1 = \rho_{sw}$. See Figure 6. This can be seen as follows. If we equate the parametrized formula for V in (11) at points $(\rho_{sw}, 0)$ and $(\rho_{sw}, \mu_Q(\overline{k}))$ and solve for $\mu_Q(\overline{k})$, we get

$$\mu_Q(\overline{k}) = 2\left(|f_s^d| - |f_{sw}|\right)\frac{k_2}{m_1}\frac{Q_1}{Q_1 + \frac{\overline{k}k_1}{m_1}Q_3} . \qquad (13)$$

[1]Theorem 4.19 actually gives three conditions, but one of them, that $v_2 \in \mathcal{O}$, is automatically met, so we omit it.

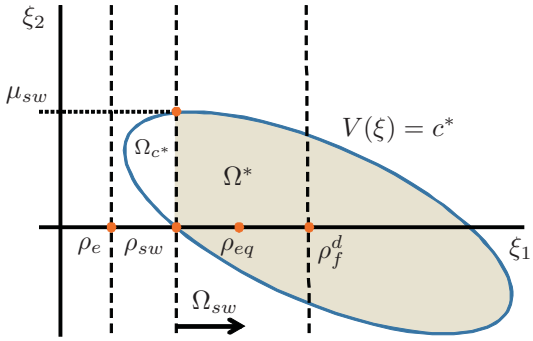

Fig. 6: The level set $V(\xi) = c^*$ and invariant Ω^* of Lemma 4.2

Now observe that $0 < \frac{Q_1}{Q_1 + \frac{\overline{k}k_1}{m_1}Q_3} < 1$, and that $\lim_{Q_1\to\infty} \frac{Q_1}{Q_1 + \frac{\overline{k}k_1}{m_1}Q_3} = 1$. Based on this observation we define the

$$\overline{\mu} := \lim_{Q_1\to\infty} \mu_Q(\overline{k}) = 2(|f_s^d| - |f_{sw}|)\frac{k_2}{m_1} . \qquad (14)$$

Clearly $\overline{\mu}$ is the least upper bound of $\mu_Q(\overline{k})$; that is, for every $\overline{k} \in [\overline{k}_{min}, \overline{k}_{max}]$, $\mu_Q(\overline{k}) \in (0, \overline{\mu})$.

Based on the foregoing, we have the following result.

Lemma 4.2: We are given (6f), f_s^d and f_{sw} with $|f_s^d| > |f_{sw}|$, $\rho_e \in [\rho_{emin}, \rho_{emax}]$, $\overline{k} \in [\overline{k}_{min}, \overline{k}_{max}]$, and $\overline{\mu}$ from (14). Suppose that $\mu_{sw} \in (0, \overline{\mu})$ is given. Let $Q = \left[\begin{smallmatrix} Q_1 & Q_2 \\ Q_2 & Q_3 \end{smallmatrix}\right]$ with $0 \leq Q_2 \leq 1$ and

$$Q_1 := \sqrt{\frac{\overline{k}_{max}k_1}{m_1}\frac{\mu_{sw}}{\overline{\mu} - \mu_{sw}}} > 0, \quad Q_3 := Q_1^{-1} . \qquad (15)$$

Then for each $\overline{k} \in [\overline{k}_{min}, \overline{k}_{max}]$ there exists a set of initial conditions

$$\Omega_0(\overline{k}) := \{\xi \in \mathbb{R}^2 \mid \xi_1 = \rho_{sw}, 0 \leq \xi_2 \leq \mu_{sw}\} \qquad (16)$$

where $\rho_{sw} = \rho_e + \frac{|f_{sw}|}{\overline{k}}$ such that $\xi(0) \in \Omega_0(\overline{k})$ implies $\xi_1(t) \geq \rho_{sw}$ for all $t \geq 0$.

Proof: Using (6g), define $\rho_f^d := \rho_e + \frac{|f_s^d|}{\overline{k}}$. Since $|f_{sw}| < |f_s^d|$ we have $\rho_e < \rho_{sw} < \rho_f^d$. Since Q is symmetric, positive definite and by Assumption 4.1, A is Hurwitz, there exists P symmetric, positive definite such that $A^TP + PA = -Q$. We choose the Lyapunov function $V(\xi) = (\xi - \xi_f^d)^T P(\xi - \xi_f^d)$ and we have $\dot{V} = -(\xi - \xi_f)^T Q(\xi - \xi^f) < 0$ for $\xi \neq \xi_f^d$. Define the sets

$$\begin{aligned} \Omega_{sw}(\overline{k}) &:= \{\xi \in \mathbb{R}^2 \mid \xi_1 \geq \rho_{sw}\} \\ \Omega_{c^*} &:= \{\xi \in \mathbb{R}^2 \mid V(\xi) \leq c^*\} \\ \Omega^*(\overline{k}) &:= \Omega_{c^*} \cap \Omega_{sw}(\overline{k}) , \end{aligned}$$

where $c^* := V((\rho_{sw}, 0))$. See Figure 6. We claim that $\Omega^*(\overline{k})$ is positively invariant under (6f). We already know that Ω_{c^*} is positively invariant. We also have that $\dot{\xi}_1 = \xi_2 \geq 0$ for all $\xi \in \partial\Omega_{sw}(\overline{k}) \cap \Omega^*$, since $\xi_2 \geq 0$. Combining with the positive invariance of Ω_{c^*}, we get $\Omega^*(\overline{k})$ is positively invariant.

Now we recall from the discussions above that $\partial\Omega_{sw}(\overline{k}) \cap \Omega^*(\overline{k})$ is a segment from $(\rho_{sw}, 0)$ to $(\rho_{sw}, \mu_Q(\overline{k}))$ where

$\mu_Q(\overline{k})$ is given in (13). Moreover, we claim $\mu_Q(\overline{k}) \in [\mu_{sw}, \overline{\mu})$. In particular, using (13), (14), and $Q_3 = Q_1^{-1}$, we have

$$\mu_Q(\overline{k}) = \overline{\mu}\frac{Q_1^2}{Q_1^2 + \frac{\overline{k}k_1}{m_1}}. \tag{17}$$

Since $0 < \frac{Q_1^2}{Q_1^2+\frac{\overline{k}k_1}{m_1}} < 1$, then $\mu_Q(\overline{k}) < \overline{\mu}$. Second, using (15) and $\overline{k}_{max} \geq \overline{k}$, we have

$$\mu_Q(\overline{k}) = \overline{\mu}\frac{Q_1^2}{Q_1^2 + \frac{\overline{k}k_1}{m_1}} \geq \overline{\mu}\frac{Q_1^2}{Q_1^2 + \frac{\overline{k}_{max}k_1}{m_1}} = \mu_{sw}.$$

This proves the claim. Because $\mu_Q(\overline{k}) \in [\mu_{sw}, \overline{\mu})$, it follows that if $\xi(0) \in \Omega_0(\overline{k}) \subset \partial\Omega_{sw}(\overline{k}) \cap \Omega^*(\overline{k})$, then by the invariance of $\Omega^*(\overline{k})$, $\xi(t) \in \Omega^*(\overline{k})$ for all $t \geq 0$. In particular, $\xi_1(t) \geq \rho_{sw}$ for all $t \geq 0$, as desired. ■

The following algorithm summarizes the steps to select the problem parameters.

Algorithm 4.1: We consider the model (6a)-(6g) with $k_e \in [k_{emin}, k_{emax}]$, $\overline{k} \in [\overline{k}_{min}, \overline{k}_{max}]$, and $\hat{\rho}_e \in [\hat{\rho}_{emin}, \hat{\rho}_{emax}]$. The model parameters m_1, m_2, k_s, r_s, k_1, k_2, and f_s^d are known. Finally, we are given the specification parameters ρ_0 and μ_1.

1) Select a switching force threshold f_{sw}, where $|f_{sw}| < |f_s^d|$.
2) Compute $\overline{\mu} = 2|f_s^d - f_{sw}|\frac{k_2}{m_1}$. Choose μ_{sw} such that $0 < \mu_{sw} < \overline{\mu}$.
3) Choose ρ_2 according to $\rho_2 > \rho_{emax} + \frac{|f_{sw}|}{\overline{k}_{min}}$, the maximum possible value of $\rho_s w$.
4) Select the velocity parameter μ_2 such that $\mu_{sw} < \mu_2 < \mu_1$. Compute the position $\rho_1 = \rho_{emin} + (\rho_2 - \rho_{emin})\frac{\mu_{sw}-\mu_2}{\mu_{sw}}$ so that $\mathcal{P}^3$ is a simplex with vertices $v_0^3 = (\rho_1, \mu_2)$, $v_1^3 = (\rho_1, 0)$, $v_2^3 = (\rho_2, 0)$.
5) Select the position ρ_3 such that $\rho_0 < \rho_3 < \rho_1$.

The algorithm provides all vertices of the polytope $\mathcal{P}$. We then partition $\mathcal{P}$ into five polytopes $\mathcal{P}^i$, $i = 1, \ldots, 5$. Reach controllers $u_{rcp}^i(\xi)$, $i = 1, \ldots, 5$ are specified on each polytope $\mathcal{P}^i$ so that $\mathcal{P}^1 \xrightarrow{\mathcal{P}^1} \mathcal{F}_0$, $\mathcal{P}^2 \xrightarrow{\mathcal{P}^2} \mathcal{F}_1$, $\mathcal{P}^4 \xrightarrow{\mathcal{P}^4} \mathcal{F}_3$, and $\mathcal{P}^5 \xrightarrow{\mathcal{P}^5} \mathcal{F}_2$. For $\mathcal{P}^3$, u_{rcp}^3 will be designed according to Lemma 4.1. Collectively, all RCP controllers u_{rcp}^i will be denoted by u_{rcp}. The overall switching controller is given as follows:

$$u(\xi) = \begin{cases} u_{rcp}^i(\xi), & \xi \in \mathcal{P}^i, i \in \{1,2,4,5\} \\ u_{rcp}^3(\xi), & \xi \in \mathcal{P}^3 \text{ and } |f_s| < |f_{sw}| \\ u_f, & |f_s| \geq |f_{sw}|. \end{cases} \tag{18}$$

The following is the main result of the paper.

Theorem 4.1: Consider the systems (6a) - (6f) and the polytope $\mathcal{P}$ whose vertices are determined by the Algorithm 4.1. Consider the controller $u(\xi)$ given in (18). The closed-loop system satisfies the following:

(i) For all $\xi(0) \in \mathcal{P}^1$, $\xi(t) \to (\rho_f^d, 0)$ as $t \to \infty$; correspondingly the steady state contact force is f_s^d.
(ii) The controller (18) switches from reach control u_{rcp} to force control u_f only once.

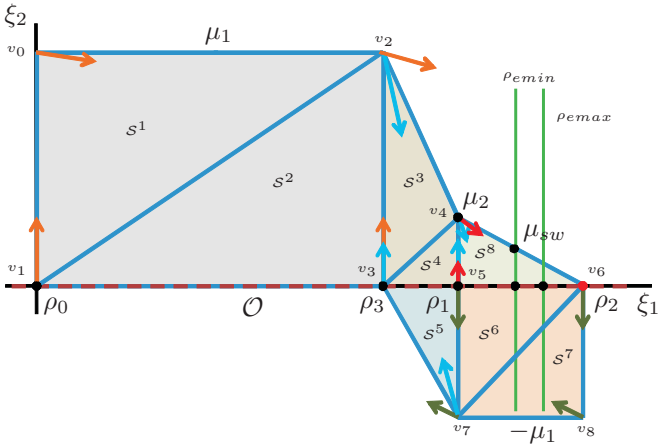

Fig. 7: The triangulated state space with desired closed-loop velocity vectors at the vertices.

(iii) Impact with the environment occurs with a velocity bounded by μ_{sw}.

Proof: It can be easily verified using the results in [6], [11] that there exist $u_{rcp}^i(\xi)$, $i = 1, 2, 4, 5$ such that $\mathcal{P}^1 \xrightarrow{\mathcal{P}^1} \mathcal{F}_0$, $\mathcal{P}^2 \xrightarrow{\mathcal{P}^2} \mathcal{F}_1$, $\mathcal{P}^4 \xrightarrow{\mathcal{P}^4} \mathcal{F}_3$, and $\mathcal{P}^5 \xrightarrow{\mathcal{P}^5} \mathcal{F}_2$.

On $\mathcal{P}^3$, Lemma 4.1 provides $u_{rcp}^3(\xi)$ that guarantees that trajectories of the non-contact system (6a) arriving in $\mathcal{P}^3$ from $\mathcal{P}^2$ reach a state when $\xi_1 \geq \rho_{emax}$. Thus, necessarily contact is made with the environment and the model switches to (6b). Lemma 4.1 further shows that under u_{rcp}^3, trajectories of (6b) reach the switching boundary $\Gamma_{sw}(\overline{k})$ when $f_s = f_{sw}$. According to (18), the controller then switches to u_f and the model reverts to (6f). In step 4 of the algorithm ρ_1 is selected so that $(\rho_{emin}, \mu_{sw}) \in \partial\mathcal{P}^3$ and since $\Gamma_{sw}(\overline{k})$ lies to the right of the $\xi_1 = \rho_{emin}$ line, we have that $\Gamma_{sw}(\overline{k}) \subset \Omega_0(\overline{k})$. Then by Lemma 4.2, trajectories of (6f) remain in a region of the state space when $f_s \geq f_{sw}$ and so the controller (18) can never switch back to u_{rcp}. This proves (ii). Also (i) follows since u_f guarantees that f_s reaches a steady-state of f_s^d. Finally, the first (and only) impact with the environment occurs at some time $\overline{t} > 0$ when $\xi(\overline{t}) \in \mathcal{P}^3$ and $\xi_1(\overline{t}) = \rho_{sw}$. But then by design (see Figures 4 and 5, $\xi_2(\overline{t}) \leq \mu_{sw}$, which proves (iii). ■

V. Control Design

In this section we solve Problem 3.1. The parameters of the problem are: $l_1 = 8$m, $l_2 = 7$m, $m_1 = 5000$kg, $m_2 = 40$kg, $r_s = 0.05$m, $k_s = 10^7$N/m, $k_e \in [10^5, 10^6]$N/m, $\bar{k} \in [9.901(10^4), 9.901(10^5)]$N/m, $\hat{\rho}_e \in [10.05, 10.07]$m, $k_1 = 1.1$, $k_2 = 0.11$, $f_s^d = -150$N, $\rho_0 = 0$m, and $\mu_1 = 0.35$m/s. Then from Algorithm 4.1 we select or calculate in order: $f_{sw} = -15$N, $\overline{\mu} = 5.94$mm/s, $\mu_{sw} = 5.5$mm/s, $\rho_2 = 11.0205$m, $\mu_2 = 6.6$mm/s, $\rho_1 = 9.8$m, and $\rho_3 = 9.3$m.

We perform the reach control design using (6a) for no contact. First, $\mathcal{P}$ is partitioned using the triangulation $\mathcal{T} = \{\mathcal{S}^1, \ldots, \mathcal{S}^8\}$ consisting of eight 2D simplices as shown in Figure 7. The vertices of $\mathcal{P}$ are $v_0 = (0, 0.35)$, $v_1 = (0, 0)$, $v_2 = (9.3, 0.35)$, $v_3 = (9.3, 0)$, $v_4 = (9.796, 0.0066)$, $v_5 = (9.796, 0)$, $v_6 = (11.0205, 0)$, $v_7 = (9.796, -0.35)$, and

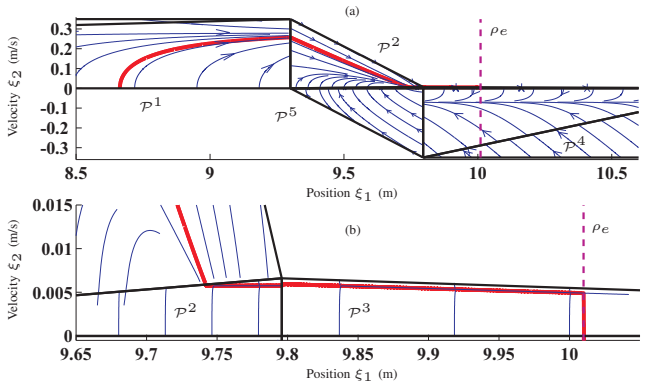

Fig. 8: Closed-loop vector field under u_{rcp} on $\mathcal{P}$ with a sample closed-loop trajectory.

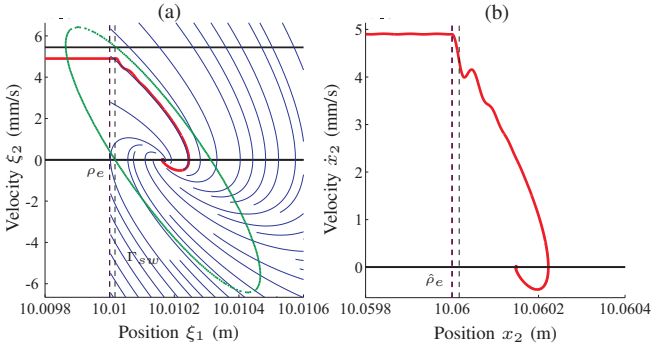

Fig. 9: Closed-loop vector field under force control u_f. when $k_e = k_{emax}$.

$v_8 = (11.0205, -0.35)$. According to the temporal sequence, red arrows in Figure 4 mark exit facets of each $\mathcal{P}^j$ in order to drive trajectories into $\mathcal{P}^3$ (in which an equilibrium is created at v_6). The arrows in Figure 7 depict desired closed-loop velocities to be achieved at the vertices. Some vertices have multiple vectors; in particular the resulting piecewise affine feedback is continuous for transitions between $\mathcal{P}^2$ and $\mathcal{P}^5$, and discontinuous for all other transitions.

Let $u_i^j \in \mathbb{R}^m$ denote the control value at vertex v_i, $i = 1, \ldots, 8$, of region $\mathcal{P}^j$, $j \in \{1, ..., 5\}$. Following the method of [2], the u_i^j are selected to satisfy the so-called invariance conditions; see [2] for details. Using equation (8) of [5], the following affine reach controllers are synthesized: $u_{rcp}^1 = [0 \ \ -3571]\xi + 1000$, $u_{rcp}^2 = [0 \ \ -3571]\xi + 1000$, $u_{rcp}^3 = [-1093 \ -5000]\xi + 10664$, $u_{rcp}^4 = [0 \ -87120]\xi + 500$, $u_{rcp}^5 = [-1159 \ -4143]\xi + 11283$, $u_{rcp}^6 = [0 \ -7143]\xi - 500$, $u_{rcp}^7 = [0 \ \ -7143]\xi - 500$, and $u_{rcp}^8 = [-424 \ \ -87300]\xi + 4667$. Finally the overall hybrid controller is constructed from the reach controllers $u_{rcp}^i(\xi)$, $i = 1, ..., 8$ and force controller u_f given by (6e).

We simulated the closed-loop system with $k_e = k_{emax} = 10^6$N/m, $\bar{k} = \overline{k}_{max} = 9.901(10)^5$N/m, and $\hat{\rho}_e = 10.06$m. In Figure 8(a) the reach controller u_{rcp} drives the states of the end effector from rest in $\mathcal{P}^1$ through to $\mathcal{P}^2$. In Figure 8(b) $\mathcal{P}^3$ is shown in more detail where the states arrive from $\mathcal{P}^2$ and the position $\rho_e = 10.01$m is reached (marked by the dashed line). The impact velocity is 4.9mm/s, well below the designed maximum $\mu_{sw} = 5.5$mm/s. In Figure 9, u_{rcp} drives the states to the switching line $\Gamma_{sw}(\overline{k})$, at which point a bumpless transfer to the force controller u_f occurs, and the states approach the equilibrium associated with the contact force f_s^d.

REFERENCES

[1] M.E. Broucke. Reach control on simplices by continuous state feedback. *SIAM Journal on Control and Optimization*. vol. 48, issue 5, pp. 3482-3500, February 2010.

[2] M.K. Helwa and M.E. Broucke. Monotonic Reach Control on Polytopes. *IEEE Trans. Automatic Control*. vol. 58, issue 10, pp. 2704-2709, October 2013.

[3] R. Carloni, R. Sanfelice, A. R. Teel and C. Melchiorri. A Hybrid Control Strategy for Robust Contact Detection and Force Regulation. *Proc. American Control Conference*. pp. 1461-1466, 2007.

[4] M.C. Cavusoglu, J. Yan and S. Shankar Sastry. A Hybrid System Approach to Contact Stability and Force Control in Robotic Manipulators. *Proc. 12th IEEE International Symposium on Intelligent Control*. Istanbul, July 1997.

[5] L.C.G.J.M. Habets and J.H. van Schuppen. A control problem for affine dynamical systems on a full-dimensional polytope. *Automatica*. No. 40, pp. 21–35, 2004.

[6] L.C.G.J.M. Habets, P.J. Collins, and J.H. van Schuppen. Reachability and control synthesis for piecewise-affine hybrid systems on simplices. *IEEE Trans. Automatic Control*. no. 51, pp. 938–948, 2006.

[7] O. Khatib and J. Burdick. Motion and force control of robot manipulators. *Proc of the IEEE International Conference of Robotics and Automation*. pp 1381-1386, 1986.

[8] C.W. Lee. Subdivisions and triangulations of polytopes. *Handbook of Discrete and Computational Geometry*. CRC Press Series Discrete Math. Appl., pp. 271–290, 1997.

[9] G.T. Marth, T.J. Tarn and A.K. Bejczy. Stable Phase Transition Control for Robot Arm Motion. *Proceedings of the IEEE Internatzonal Conference on Robotcis and Automation*. Atlanta, Georgia, pp. 355-362, 1993.

[10] P.R. Pagilla and B. Yu. A Stable Transition Controller for Constrained Robots. *IEEE/ASME Transactions on Mechatronics*. Vol. 6, No. 1, pp. 65-74, 2001.

[11] B. Roszak and M.E. Broucke. Necessary and sufficient conditions for reachability on a simplex. *Automatica*. vol. 42, no. 11, pp. 1913–1918, November 2006.

[12] M. Spong, S. Hutchinson, and M. Vidyasagar. *Robot Modeling and Control*. Wiley, 2006.

[13] T. Tarn, Y. Wu, N. Xi, and A. Isidori. Force Regulation and Contact Transition Control. *IEEE Control Systems Magazine*. Vol. 16, pp. 32-40, 1996.

[14] R. Volpe and P. Khosla. A theoretical and experimental investigation of impact control for manipulators. *Interational Journal of Robotics Research*. Vol. 12, no. 4, pp. 351365, Aug. 1993.